Speckle Interferometry with the OCA Kuhn 22" Telescope - II

Rick Wasson

Murrieta, California
ricksshobs@verizon.net

Abstract: This paper reports Speckle Interferometry measurements of double stars made during 2017, using the Kuhn 22-inch telescope of the Orange County Astronomers, a ZWO ASI 290MM CMOS camera, and four interference filters. Observations are reported for 71 systems. Targeted separations ranged from 0.3" to 3.0", but wider components of several multiple systems were also measured. Astrometric data reduction utilized the REDUC and Speckle Tool Box programs, and bispectrum analysis was also done for all stars. Equipment, data acquisition, astrometric and photometric data reduction and analyses are described. Results for several stars are discussed in detail.

Introduction

The author is a member of the Orange County Astronomers (OCA), one of the largest and most active amateur astronomy clubs in the United States. One of the many privileges of OCA membership is the use, after completing a training course, of the Kuhn 22-inch (0.56 meter) f/8 Cassegrain telescope. The observatory is located at the club's Anza observing site in the hills about 15 miles northeast of Mount Palomar Observatory, at 4300 feet elevation under a moderately dark sky.

The first article in this series (Wasson, 2018) reported on the beginning use of the Kuhn 22" for speckle interferometry of close double stars. This paper describes the continuing observational program, with two major improvements: (1) An improved camera, the ZWO ASI290MM with low read noise and improved near-IR sensitivity; (2) Adding Bispectrum Analysis (BSA) to the normal Autocorrelation (AC) method of speckle analysis. Only significant changes to methods and equipment from the previous paper are discussed here. The telescope and instrumentation ready for speckle interferometry are shown in Figure 1.

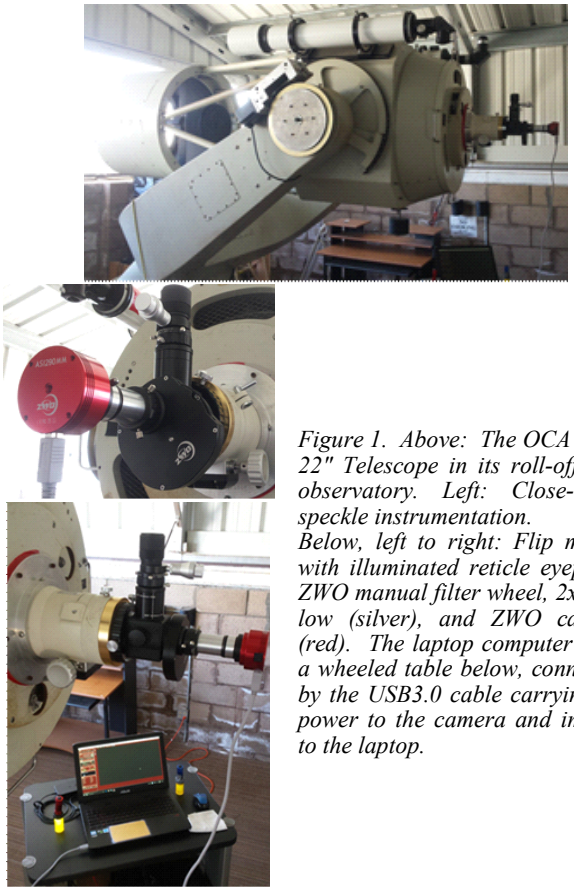

Figure 1. Above: The OCA Kuhn 22" Telescope in its roll-off roof observatory. Left: Close-up of speckle instrumentation.
Below, left to right: Flip mirror with illuminated reticle eyepiece, ZWO manual filter wheel, 2x Barlow (silver), and ZWO camera (red). The laptop computer is on a wheeled table below, connected by the USB3.0 cable carrying 5V power to the camera and images to the laptop.

Camera Upgrade

All observations in this paper used a ZWO ASI290MM high-speed monochrome camera, which has a Sony IMX290LLR back-illuminated CMOS detector with 2.90 μ square pixels in a 1936x1096 array,

and a rolling shutter. This un-cooled camera was chosen because the back-illuminated design, new technology for CMOS cameras, gives improved sensitivity in the near-IR spectral region; because the read noise is very low (~1e- rms depending on gain); and because this high-tech unit is available for only about $400US. It has a high-speed USB3.0 interface (more than 30 fps full frame), providing 12-bit images. The Quantum Efficiency (QE) is believed to be about 70% peak at 600 nm, and still 24% at 900nm.

Because of the small pixels, less magnification is required to reach the optimum speckle image scale – about 7 to 8 pixels across the Airy disk diameter (Rowe, 2016) – a good compromise between more pixel sampling and less light available per pixel. Therefore, a simple 2x Barlow is used on the Kuhn 22", providing f/16, a plate scale of about 0.066 arc-sec/pixel, and about 8.8 pixels across the Airy disk at 650nm wavelength. The speckle field is small - about 2.2'x1.2' - but is adequate for close double stars, and large enough for easy centering with an illuminated reticle eyepiece.

Filters

A ZWO manual filter wheel was used, housing the three 1¼-inch filters already in hand; a longer wavelength IR-pass filter (IR807) was added to make use of the better near-IR QE of the back-illuminated sensor, for observations of very red stars (Serot et al, 2018). Table 1 gives the characteristics of the four interference filters used for the observations reported here. These filters are not members of any photometric standard series, but they are economical, durable, and cover the detectable wavelength range of the camera well.

For the two long-pass filters in Table 1, asterisks indicate convolved characteristics: i.e., filter transmission times QE of the CMOS detector. The "50% Band Pass" column for these two filters is 50% cut-on transmission on the short side, but it is assumed to be 1 micron on the long side because detection is determined by the Silicon detector sensitivity limit (~1μ) rather than filter transmission.

Target Selection and Observation

Double star targets were chosen by searching the Washington Double Star (WDS) Catalog, primarily using the search tool WDS1.2 (Rowe, 2017). Input parameters include ranges for RA and Dec, primary star magnitude, magnitude difference and separation. This program also gives a list of possible reference stars within 3 degrees of the target; the list may be sorted by distance or magnitude. These are very important, time-saving features for the user, making it easy to select a suitable reference star, which should be as close to the target star as possible in terms of location, magnitude and color (spectral type). A reference star was usually observed immediately after every double star.

The target search parameters generally employed were:

- 0.3" < Separation < 3.0".
- Primary star brighter than magnitude 11.
- Declination between +68° and -2° (i.e.,observatory latitude ~33° +/- 35°).

Special consideration was given to binary stars which already have orbital solutions, in the hope of providing additional speckle measurements for refining the orbits. For some stars, especially those with orbits, detailed information was found at the Italian website Stelle-Doppie (Sordiglioni, 2016), including SAO number, orbital period, and current orbit ephemerides for Separation (ρ) and Position Angle (θ).

A "master" Target List was built as an EXCEL workbook, covering the entire RA range in spreadsheets of 2 hours each. The WDS orbit plots were also copied and hyper-linked into the spreadsheets for quick reference. For each observing run, a copy of the workbook was made, to serve as the observing log by entering observation date, sequence numbers, filters and notes into the spreadsheets in real time.

A sequence of 1000 frames was acquired for most

Table 1. Filter characteristics. These interference filters typically have a sharp rise and fall of about 10 nm width, and a high, nearly constant transmission plateau (95+%). The "IR742" and "IR807" filters are long-pass IR transmission filters.

Filter	Manufacturer Name	50% Band Pass (nm)	Center Wavelength (nm)	Width (nm)	Peak Transition
G	Baader G (LRGB Series)	495 - 575	534	80	96%
R	Baader R (LRGB Series)	585 - 690	636	105	98%
IR742	Astronomik ProPlanet 742	736 – *	844 *	260 *	56% *
IR807	Astronomik ProPlanet 807	800 – *	885 *	200 *	44% *

double and reference stars; more than one sequence was recorded for some doubles having a faint secondary star, with the intention to improve S/N. Stars were generally observed at zenith angles less than about 35 degrees, because an atmospheric dispersion corrector was not used; it has been found that for larger zenith angles atmospheric dispersion "smearing" becomes noticeable for the moderate-width filters of Table 1, possibly degrading separation and position angle accuracy.

Acquisition and Analysis Software

All data acquisition, processing and analysis was performed on a laptop computer with Intel i7 quad processors, running Windows 10. FireCapture 2.6 (Edelmann, 2015) software was used for all data acquisition. This very versatile program, designed primarily for planetary imaging, can be used with many types of astronomy cameras, easily handles fast USB3.0 data speeds from the camera, and can store raw data frames as FITS files, a convenient format for Speckle data processing in both REDUC (Losse, 2015) and Speckle Tool Box (STB) software (Rowe & Genet, 2015).

The Drift Calibration method (Wasson, 2018) was used to calibrate each night's data for Plate Scale and Camera Orientation on the sky. Multiple drifts were made throughout the night - typically several drifts on each of several bright reference stars; the average of all drift results was used to reduce all the speckle data for that night.

Each drift sequence was first edited in REDUC to delete frames where the star was absent from the field, not moving, or overlapped the edge. A convenient Drift Calibration tool is part of the STB data reduction program (Harshaw, Rowe and Genet, 2017). Plate scale was about 0.0662 arc-sec/pixel. Standard deviation of plate scale calibrations for the 6 nights of observation ranged from 0.00022 to 0.00044"/pixel. Standard deviation of the camera orientation on the sky ranged from 0.13 to 0.37 degree.

STB version 1.13 software (Rowe, Genet, Wasson, 2019) was employed for all speckle data analysis. It includes tools for both normal speckle AC and triple correlation BSA. The first step of processing was assembly of each sequence of double or reference star images into FITS cube format. STB has a simple-to-use tool to create the FITS cubes, which centers each frame on the star and, if desired, crops all frames to a smaller size, to speed up processing time and reduce file storage space. The original speckle frames were a 512x512 pixel region of interest (ROI) near the center of the larger camera field of view, allowing plenty of room for approximate centering and movement from seeing and telescope tracking errors. In creating the FITS cubes, the field was cropped to 128x128 pixels (or 256x256 for wide doubles), but the original frames are not altered.

Dark frames were generally not recorded or used in AC or BSA processing. Of course, if dark frames were to be used, they must be taken with exactly the same camera ROI as the speckle frames, and the master dark must be subtracted from all *original* speckle frames - before creating a FITS cube with smaller cropped frames. This is because these smaller images are randomly positioned to follow the star movements and center it, losing registry with both original and dark frames.

Normal speckle AC processing, including deconvolution with a reference star, was first performed for all the double stars; results were written to a .csv (spreadsheet) file – another convenient STB feature. The latest WDS observation or orbit ephemerides was used to select the correct θ quadrant from the two peaks given by the AC solution. The same set of double and reference star FITS cubes were then used for BSA in STB1.13, and these results were copied into the AC spreadsheet for comparison.

Bispectrum Analysis

Bispectrum analysis – also known as triple-correlation – is an extension of the AC speckle analysis technique; ρ, θ and Δmagnitude of double stars down to near the diffraction limit can be measured. BSA has been used by professional astronomers for some time (Horch, et al, 1999). STB1.13 became available to amateur speckle observers in 2017 for experimental testing (Serot, et al, 2018), and is expected to be available by request from the author in 2019.

Two inherent mathematical limitations arise from AC processing: (1) the 180° uncertainty of θ, because of the two identical secondary peaks in the AC; and (2) amplitudes of the AC peaks have no relationship with star brightness, so magnitudes of the components cannot be measured.

The goal of BSA is to overcome the limitations of AC through more advanced mathematical processing. The first step is calculation of the bispectrum from the average of the triple correlation of all individual images; this four-dimensional BSA processing takes roughly 10 times more CPU time than that for the AC power spectrum alone. The second step, using the STB "Bispectrum Phase Reconstruction" tool, is an iterative procedure under control of the user, which yields a reconstructed diffraction-limited image with atmospheric distortion removed. Processing with the bispectrum of a reference (single) star serves to reduce optical and atmospheric aberrations which are common to both double and reference images, just as it does for an autocorrelation. Mathematical filtering techniques may also

Speckle Interferometry with the OCA Kuhn 22" Telescope - II

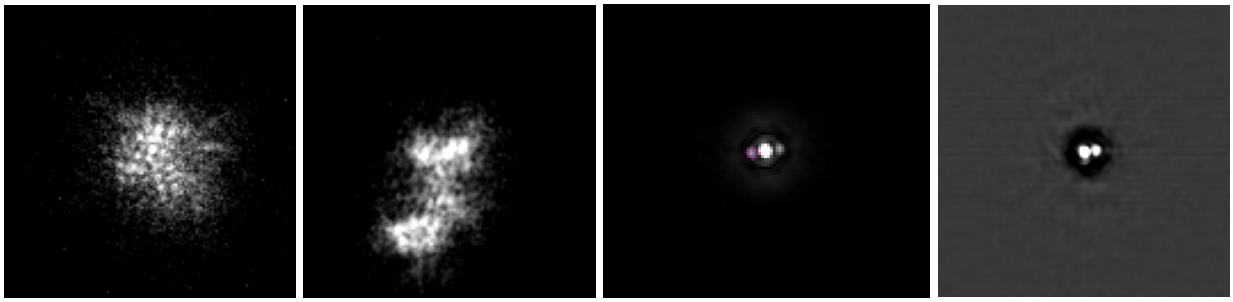

Figure 2. An example of processing results for the double star 11190+1416 STF1527, WDS magnitudes 7.01/7.99, Δmag = 0.98, spectrum F9V. 3000 frames were recorded, using 0.030 sec exposures, in the G filter. Left to Right: Two representative raw speckle frames; the autocorrelation (ρ = 0.312", θ = 277.42 deg.); the BSA reconstructed image (ρ = 0.338", θ = 277.46 deg, Δmag = 1.16).

be applied to improve the S/N and clarity of the image. Examples of the AC and BSA reconstructed image for a typical double star are shown in Figure 2.

Bispectrum ΔMagnitudes

STB 1.13 has a convenient tool for measuring ρ, θ and Δmagnitude from the BSA reconstructed image. The user chooses circular photometry apertures for the primary star, secondary star and background. Measurement of Δmagnitude must use the *same* photometry aperture for both the primary and secondary components, but not necessarily for the background. The importance of using the same star apertures is illustrated by the photometric "growth curve" in Figure 3. The measured magnitude of a star obviously depends on the aperture radius, but noise limits the maximum useful radius. Fortunately, stars of different brightness have the *same* point spread function (PSF), differing only in flux amplitude. The same aperture captures the same *proportion* of light for both stars, giving the correct Δmagnitude even though not all the light is included. The aperture should be sized for the fainter star, limited to the radius where noise begins to be added faster than starlight.

In practice, speckle photometry of close double stars is generally less accurate than conventional wide-

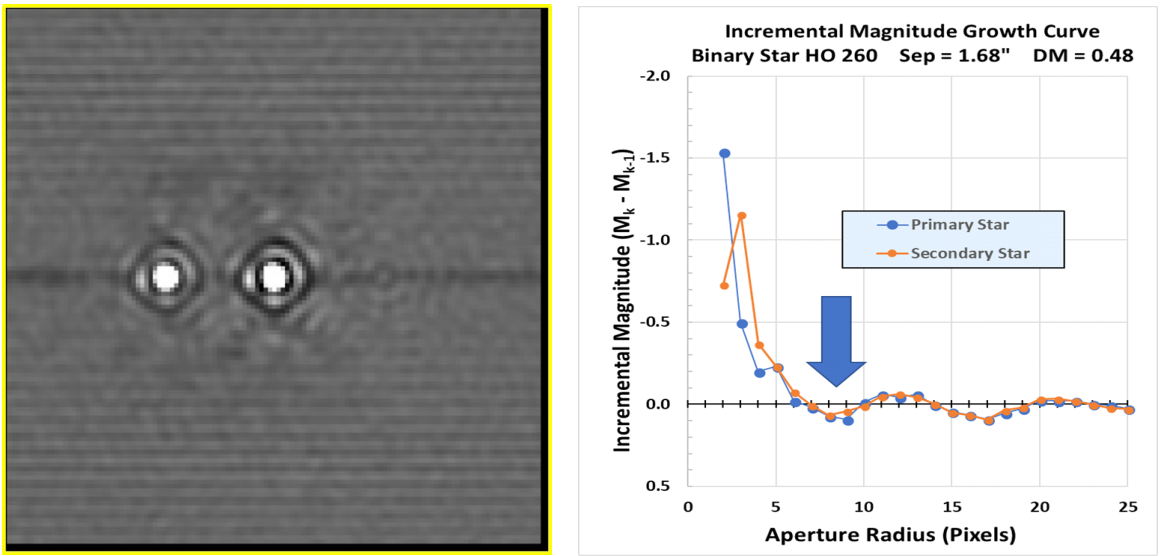

Figure 3. Left: BSA reconstructed image of the binary HO260, ρ = 1.68". The image is stretched to show low-amplitude detail; the Airy disk, 1st diffraction ring, and parts of the 2nd ring are clearly visible. Residual low-level fixed pattern noise also becomes visible as horizontal lines. Right: The magnitude vs aperture "growth curve." Brightness grows as radius of the photometric aperture increases, but the growth curve is shown here as the declining difference in magnitude for a one-pixel increase in radius (valid only for Radius>2). This format, which is analogous to the Point Spread Function, amplifies the curve sensitivity so that the shallow diffraction rings can be clearly seen. PSF of the two stars is the same in radial extent, even though their brightness is different by 0.5 magnitude. The Rayleigh criterion (blue arrow) is at the minimum of the 1st ring.

field CCD photometry. Four obvious challenges are: (1) BSA images are mathematical reconstructions (not original recordings of flux), so noise can affect every step of reconstruction processing; (2) short exposures limit the S/N of faint stars, (3) the two nearby PSFs may overlap each other, similar to crowded-field photometry; (4) diffraction rings of separated stars may still overlap and interfere with the companion PSF, adding "signal" to the wrong star.

No attempt has been made here to transform the non-standard filter Δmagnitude results to any standard photometric system, but work is underway to investigate that possibility. Further issues associated with measurement of Δmagnitudes are discussed in Serot, et al, 2018.

Speckle Measurement Quality

Quality of the speckle measurements was not statistically evaluated. Usually only one sequence was recorded, consisting of 1000 frames; for systems with large Δmagnitude, multiple sequences were sometimes taken. However, no statistical information was calculated because all the available frames were combined into one large FITS cube for AC and BSA processing, with the intention of maximizing S/N.

A *qualitative* figure of merit was assigned to each measurement, as shown in Table 2, with values rated from 1 (good) to 7 (not useable). The same criteria were used for both AC and BSA results. When measuring ρ and θ in STB, most doubles were bright and wide enough to yield very repeatable "solid" solutions - meaning that the peaks (centroids) of the AC or BSA image were accurately located and did not shift when moving the measurement aperture slightly. Observations with mild atmospheric dispersion, causing slightly "smeared" AC or BSA image peaks, were assigned quality 2. Close or faint secondary measurements were given values of 3 or 4, respectively, if the measurements were still "solid."

For very close and/or faint doubles, where measurements were marginal and difficult, higher numbers were assigned. Values of 5 are considered uncertain, because the secondary peak was not clearly separated from the central peak, making its centroid location questionable. Values of 6 are also uncertain because the faint secondary peak was distorted by, or not clearly distinguishable from, background noise or primary contamination. A value of 7 indicates that no reasonable measurement was possible. In Tables 2 and 3 below, those measurements having poor quality of 5, 6 or 7 are flagged in color.

Double Star AC and BSA Measures

Speckle measurements with the OCA Kuhn 22-inch telescope reported in Table 3 were made from March through October 2017.

Double stars with separation up to 3" were targeted, but several of these are multiple systems in which an additional component, having a wider separation (up to about 6"), was also measured. One reference star was inadvertently chosen which happened to be the wide double STF2398 (ρ ~ 8"); therefore, it was also measured by using the bright primary of the original, well-resolved double (BU385AB) in the role of "reference" star. Such wide components were certainly not within the same isoplanatic patch - therefore, speckle techniques do not strictly apply. However, the same speckle processing was used for them, and the results seem reasonable.

It must be noted that the observations of 2017 October 15 (2017.789) were taken at half the normal plate scale (0.1308 instead of 0.066) because the 2x Barlow was inadvertently left out of the optical assembly. Therefore, these observations are somewhat pixelated, compromising the accuracy of ρ, θ, and Δmagnitude measurements, which are considered approximate. An

Table 2. Qualitative Figure of Merit for ρ and θ measurements. A Figure of Merit code number is given for each measurement in Table 3.

Figure of Merit	Notes Related to Quality of the Observations
1	Bright, clear AC or BSA image. Solid measurement.
2	Some distortion of fringes or peaks, but measurement solid.
3	Close, but measurement clear, solid.
4	Companion faint, but measurement clear, solid.
5	Very close. Measurement uncertain.
6	Companion very faint. Measurement uncertain.
7	Companion too close or faint. Measurement NOT valid.

Speckle Interferometry with the OCA Kuhn 22" Telescope - II

Table 4. Statistics for the differences between AC and BSA measurements.

	θ (deg)	ρ (arc-sec)
Average (AC-BSA)	-0.05	-0.007
Standard Deviation	1.16	0.021
Error of Mean	0.13	0.002

example is given for the star 00308+4732 BU394AB below. Only stars whose separation is greater than 0.6", about twice the normally achievable resolution, are reported for that date.

The differences between AC and BSA are summarized in Table 4, for the 81 measurements of Table 3 which have results from both methods. The average values for θ and ρ differences are close to zero, as they should be since both techniques were always applied to the same original image data, validating that the differences are random. Thus, it is believed there are no significant systematic errors in the AC or BSA astrometry. The standard deviations may be a rough indication of the overall uncertainty of the measurements of Table 3: θ ~ ± 1 degree and ρ ~ ± 0.02".

Discussion of Selected Double Stars

Many of the stars observed in Table 3 are binaries with at least a preliminary orbit. Some were found to have large O-C values for ρ or θ, relative to the orbit ephemerides. In addition, a few stars had large movement from relatively few prior measures. Some of these stars are discussed below, as are observational circumstances that may affect the measurements.

In all Figures 4 through 15, where AC and BSA images are shown, the orientation is North up and East left. The corresponding WDS orbit plots, however, are shown in their customary rotated orientation.

The binary star **00308+4732 BU394AB** is shown in Figure 4. As noted above, this star was observed on

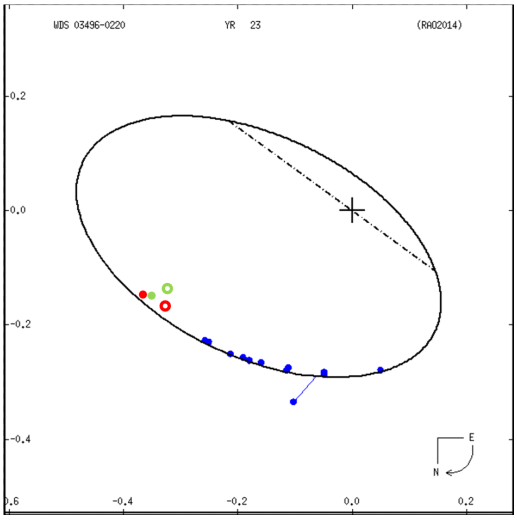

Figure 5. YR 23 orbit plot from the WDS 6th Orbit Catalog. The new AC points from Table 3 are shown as open green and red circles for the G and R filters, respectively. The new BSA points are solid green and red circles respectively, for the G and R filters.

2017 October 15, without the 2x Barlow installed; therefore, the AC and BSA images are pixelated and the measurement accuracy is degraded.

The WDS orbit of binary **03496-0220 YR23** (Riddle, et al, 2015) having a period of 54 years is shown in Figure 5. Although not resolved by Hipparcos, it was classified as "suspected non-single." Regular speckle observations were begun in 2000 with the 3.5-meter WIYN telescope at Kitt Peak (Horch, et al, 2002), and all observations to date have been made with speckle or adaptive optics techniques. YR23 is a triple system; one of the visual components is an unresolved spectroscopic binary.

The new data points from Table 3 have been added to the WDS orbit plot in Figure 5. These points, which are approaching the diffraction limit of the 22-inch telescope, obviously have considerably more scatter than

(Text continues on page 281)

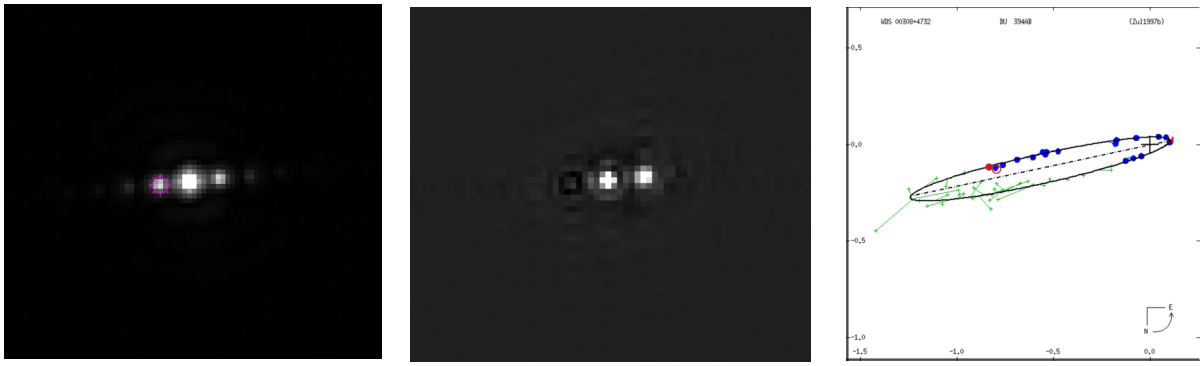

Figure 4. AC and BSA images of BU394AB in the R filter, showing the pixilation caused by observation at inadequate pixel scale (0.1308"/pixel). Left: AC. Middle: BSA reconstructed image. Right: WDS orbit plot with Table 3 measures added as red circles, AC open, and BSA solid.

Speckle Interferometry with the OCA Kuhn 22" Telescope - II

Table 3. Speckle measurements in 2017, using the OCA Kuhn 22-inch telescope, ZWO ASI290MM CMOS camera, and interference filters. The columns are: Besselian observation date, WDS RA and Dec, WDS discovery designation, WDS magnitudes of primary/ secondary, WDS magnitude difference (secondary-primary), WDS spectrum, observation filter (Table 1), AC position angle observed (deg), AC separation observed (arc-sec), BSA position angle observed (deg), BSA separation observed (arc-sec), BSA magnitude difference observed (secondary-primary), and qualitative figure of merit (Table 2) for AC/BSA.

Date	WDS	Discovery	mA / mB	DMag	Spectrum	Filter	AC θ	AC ρ	BSA θ	BSA ρ	BSA ΔMag	Qual
2017.789	00308+4732	BU 394AB	8.49 / 8.77	0.28	G0	R	278.52	0.809	278.28	0.840	0.17	1 / 1
2017.789	00504+5038	BU 232AB	8.46 / 8.79	0.33	F5	R	255.49	0.914	255.51	0.927	0.20	1 / 1
2017.170	03496-0220	YR 23	7.73 / 8.29	0.56	G0	G	292.56	0.351	296.37	0.366	0.58	2 / 2
2017.170	03496-0220					R	293.22	0.379	292.13	0.394	0.17	2 / 2
2017.170	03503+2535	STT 65	5.73 / 6.52	0.79	A2V + A5V	G	201.84	0.440	202.01	0.449	0.44	2 / 2
2017.170	04199+1631	STT 79	7.26 / 8.62	1.36	F9V	G	7.66	0.546	7.21	0.549	1.15	1 / 1
2017.170	04199+1631					R	6.79	0.524	8.05	0.555	1.11	2 / 2
2017.257	06214+0216	A 2667	6.63 / 8.02	1.39	A4.5V	G	279.70	0.319	279.37	0.324	0.95	3 / 3
2017.214	06573+5825	STT 159AB	4.45 / 5.50	1.05	G8III + F8V	IR742	234.74	0.696	235.60	0.717	1.55	1 / 1
2017.257	07401+0514	STF1126AB	6.55 / 6.96	0.41	A0III	G	175.54	0.870	175.82	0.883	0.53	1 / 1
2017.257	07401+0514					R	175.62	0.870	175.80	0.880	0.55	1 / 1
2017.170	07417+0942	STF1130	8.76 / 9.48	0.72	G0	R	61.79	0.522	62.03	0.528	0.49	1 / 1
2017.170	07573+0108	STT 185	7.3 / 7.1	0.20	F7V	R	19.78	0.384	19.96	0.391	0.11	1 / 1
2017.170	08041+3302	STT 187	6.94 / 8.50	1.56	A1.5V	G	337.12	0.419	336.69	0.436	0.21	1 / 1
2017.170	08044+1217	BU 581AB	8.46 / 8.83	0.37	K0V	R	217.63	0.392	219.60	0.395	0.13	1 / 1
2017.170	08044+1217					R	217.99	0.393	218.60	0.391	0.15	1 / 1
2017.170	08044+1217	BU 581AC	8.46 / 11.78	3.32	K0V	R	221.98	5.526	222.02	5.527	2.84	1 / 1
2017.170	08044+1217					R	221.96	5.498	221.95	5.535	2.60	1 / 1
2017.214	08050+5825	A 1073	9.24 / 9.89	0.65	F8	IR742	-	-	-	-	-	7 / 7
2017.170	08122+1739	STF1196AB	5.30 / 6.25	0.95	F8V	R	14.77	1.149	14.63	1.146	0.31	1 / 1
2017.170	08122+1739					IR742	14.79	1.146	14.36	1.149	0.34	1 / 1
2017.170	08122+1739	STF1196AC	5.30 / 5.85	0.55	F8V	R	61.18	6.263	61.17	6.263	0.38	1 / 1
2017.170	08122+1739					IR742	61.19	6.258	61.26	6.264	0.35	1 / 1
2017.170	08122+1739	HUT 1CaCb	6.2 / 7.1	0.90	M1	R	273.27	0.417	-	-	-	6 / 7
2017.170	08122+1739					IR742	270.79	0.464	-	-	-	6 / 7
2017.214	08231+2001	HO 525AB	9.83 / 9.89	0.06	F5	R	353.96	0.436	353.79	0.445	0.80	1 / 1
2017.214	08531+5457	A 1584	8.99 / 7.72	-1.27	G0	R	93.29	0.677	93.30	0.683	0.08	1 / 1
2017.331	08592+4803	HJ 2477AB	3.13 / 9.9	6.07	A7IV	IR807	89.76	2.418	-	-	-	6 / 7
2017.331	08592+4803	HU 628AC	3.13 / 10.1	6.97	A7IV	IR807	111.96	2.185	-	-	-	6 / 7
2017.331	08592+4803	HU 628BC	9.9 / 10.1	0.20	M1	IR807	206.17	0.915	-	-	-	4 / 7
2017.170	09006+4147	KUI 37AB	4.18 / 6.48	2.30	F3V + K0V	R	138.15	0.435	140.49	0.402	1.70	6 / 5
2017.170	09006+4147					IR742	143.78	0.480	143.70	0.452	1.74	6 / 3
2017.214	09036+4709	A 1585	4.16 / 4.54	0.38	A1V	G	283.66	0.274	284.95	0.263	0.31	5 / 5
2017.214	09179+2834	STF3121AB	7.9 / 8.0	0.10	K0	R	23.10	0.468	22.72	0.476	-0.02	1 / 1
2017.214	09186+2049	HO 43	9.31 / 9.46	0.15	F5	R	96.64	0.611	97.14	0.606	0.35	1 / 1
2017.257	09210+3811	STF1338AB	6.72 / 7.08	0.36	F2V + F4V	G	311.61	1.155	311.58	1.149	0.35	1 / 1
2017.257	09210+3811					R	311.39	1.150	311.30	1.150	0.32	1 / 1
2017.214	09260+2839	A 222	9.13 / 9.41	0.28	F8	R	4.25	0.384	4.81	0.372	0.32	1 / 1
2017.257	09285+0903	STF1356	5.69 / 7.28	1.59	F9IV	R	112.19	0.845	112.13	0.848	0.51	1 / 1
2017.214	09521+5404	STT 208	5.28 / 5.39	0.11	A2V	G	307.18	0.395	308.31	0.401	0.08	1 / 1
2017.257	09591+5316	A 1346	8.84 / 9.66	0.82	F8	R	178.10	0.570	178.26	0.607	0.99	2 / 2
2017.331	10163+1744	STT 215	7.25 / 7.46	0.21	A9IV	IR742	175.99	1.507	176.01	1.506	0.37	1 / 1
2017.331	10192+2034	STF1423	9.4 / 10.08	0.68	K0	IR742	310.96	0.726	310.77	0.713	0.98	1 / 1
2017.331	10269+1713	STT 217	7.85 / 8.58	0.73	F6V	IR742	149.04	0.827	149.27	0.832	0.35	1 / 2

Table 3 concludes on the next page.

Speckle Interferometry with the OCA Kuhn 22" Telescope - II

Table 3 (conclusion). Speckle measurements in 2017, using the OCA Kuhn 22-inch telescope, ZWO ASI290MM CMOS camera, and interference filters. The columns are: Besselian observation date, WDS RA and Dec, WDS discovery designation, WDS magnitudes of primary/secondary, WDS magnitude difference (secondary-primary), WDS spectrum, observation filter (Table 1), AC position angle observed (deg), AC separation observed (arc-sec), BSA position angle observed (deg), BSA separation observed (arc-sec), BSA magnitude difference observed (secondary-primary), and qualitative figure of merit (Table 2) for AC/BSA.

Date	WDS	Discovery	mA / mB	DMag	Spectrum	Filter	AC θ	AC ρ	BSA θ	BSA ρ	BSA ΔMag	Qual
2017.214	10279+3642	HU 879	4.62 / 6.04	1.42	G8III	R	228.41	0.531	227.62	0.530	1.26	1 / 1
2017.214	10426+0335	A 2768	6.92 / 8.45	1.53	F7V	R	241.98	0.625	242.83	0.626	1.30	1 / 1
2017.170	10454+3831	HO 532AC	9.42 / 11.76	2.34	M2	IR742	230.53	0.749	231.03	0.731	1.79	1 / 1
2017.257	10480+4107	STT 229	7.62 / 7.92	0.30	A5IV	R	257.26	0.677	257.43	0.682	0.29	1 / 1
2017.257	10544+3840	COU1746	10.70 / 10.91	0.21	K0	IR742	329.94	0.374	331.17	0.325	0.16	6 / 6
2017.331	10585+1711	A 2375	10.44 / 10.03	-0.41	G5	R	169.76	0.505	169.17	0.522	-0.40	1 / 1
2017.257	11037+6145	BU 1077AB	2.02 / 4.95	2.93	G9III	R	339.38	0.775	342.38	0.806	3.59	6 / 6
2017.331	11107+3110	HJ 2562	10.53 / 11.4	0.87	K5	IR742	221.56	0.992	221.05	1.009	0.79	1 / 1
2017.257	11182+3132	STF1523AB	4.33 / 4.80	0.47	F9V + G9V	R	164.52	1.904	164.58	1.908	0.41	2 / 2
2017.331	11190+1416	STF1527	7.01 / 7.99	0.98	F9V	G	277.42	0.312	277.46	0.338	1.16	3 / 3
2017.170	11239+1032	STF1536AB	4.06 / 6.71	2.65	F4IV	IR807	94.78	2.180	94.85	2.180	1.98	1 / 1
2017.331	11293+3025	L 11	7.22 / 10.35	3.13	F6V	IR742	277.93	1.072	276.64	1.066	2.77	4 / 4
2017.257	11308+4117	STT 234	7.45 / 8.13	0.68	F6V	R	181.23	0.404	181.05	0.431	0.18	2 / 2
2017.257	11323+6105	STT 235AB	5.69 / 7.55	1.86	F8V	R	42.58	0.929	42.95	0.931	1.43	1 / 1
2017.257	12060+6842	STF3123AB	8.01 / 7.9	-0.11	F6V	G	190.60	0.304	189.92	0.308	0.23	5 / 5
2017.257	12060+6842	STF3123AB,C	7.2 / 15.7	8.50	F6V	IR807	301.62	2.954	301.92	3.004	5.06	4 / 4
2017.331	12108+3953	STF1606	7.44 / 7.93	0.49	A8III	G	144.73	0.582	144.44	0.587	0.52	1 / 1
2017.214	12291+3123	STT 251	8.35 / 9.27	0.92	G0	R	59.79	0.727	59.58	0.731	1.15	1 / 1
2017.214	12572+0818	FIN 380	7.50 / 7.88	0.38	F5	G	-	-	-	-	-	7 / 7
2017.257	13007+5622	BU 1082	5.02 / 7.88	2.86	F2V	R	126.88	0.781	127.33	0.775	2.00	1 / 1
2017.331	13081+2657	STT 260	8.98 / 9.5	0.52	F9V	G	41.31	0.310	41.49	0.314	0.18	3 / 3
2017.331	13091+2127	HU 572	8.73 / 10.08	1.35	G5	G	332.27	0.529	333.39	0.524	1.37	1 / 1
2017.257	13198+4747	HU 644AB	9.11 / 9.87	0.76	K0	G	79.22	0.361	79.20	0.357	0.96	1 / 1
2017.331	13235+2914	HO 260	9.6 / 9.94	0.34	M0+M0.5	R	89.00	1.682	88.97	1.683	0.46	1 / 1
2017.331	13258+4430	A 1609AB	9.49 / 8.79	-0.70	K0	R	66.40	0.345	66.93	0.341	0.13	3 / 5
2017.331	13258+4430	—	—	—	—	IR807	65.85	0.394	63.03	0.336	0.43	5 / 5
2017.331	13258+4430	A 1609AC	8.33 / 13	4.67	K0	R	220.04	2.566	220.02	2.565	2.86	4 / 4
2017.331	13258+4430					IR807	219.86	2.541	220.09	2.552	2.29	4 / 4
2017.331	13284+1543	STT 266	7.97 / 8.42	0.45	F5	G	357.59	2.012	357.65	2.010	0.62	1 / 1
2017.331	13482+2248	COU 401	9.5 / 10.6	1.10	G0+G8	G	6.78	0.331	-	-	-	5 / 7
2017.331	13577+5200	A 1614	8.99 / 9.13	0.14	G5	R	299.34	1.447	299.40	1.449	0.37	1 / 1
2017.531	17366+4827	COU1922	7.72 / 9.64	1.92	F6V	G	83.29	0.348	79.34	0.375	1.34	1 / 1
2017.531	17366+4827					R	81.61	0.377	78.09	0.400	1.55	1 / 1
2017.789	20102+4357	STT 400	7.6 / 9.83	2.23	G3V	R	327.58	0.644	328.76	0.695	0.15	1 / 1
2017.789	20210+4437	A 725	9.46 / 10.23	0.77	K0	R	25.99	0.854	25.13	0.878	0.64	1 / 1
2017.789	21137+6424	H 1 48	7.21 / 7.33	0.12	G2IV+G2IV	R	244.10	0.695	242.55	0.740	0.08	1 / 1
2017.789	21148+3803	AGC 13AB	3.83 / 6.57	2.74	F3V+F7V	R	190.72	0.895	-	-	-	4 / 7
2017.789	21223+5734	A 764AB	8.23 / 10.69	2.46	G5	R	199.10	1.338	198.88	1.319	-1.84	1 / 1
2017.789	22202+2931	BU 1216	8.61 / 9.21	0.60	F5	R	276.52	0.961	275.81	0.968	0.47	1 / 1
2017.789	22281+1215	BU 701AB	7.34 / 9.62	2.28	K0V	R	175.82	0.993	178.91	1.073	2.27	1 / 1
2017.789	22514+2623	HO 482AB	7.34 / 8.29	0.95	A9V	R	13.06	0.528	12.70	0.561	0.11	1 / 1
2017.789	23075+3250	STF2978	6.35 / 7.46	1.11	A3V	R	144.47	8.356	144.61	8.344	1.12	1 / 1
2017.789	23103+3229	BU 385AB	7.44 / 8.23	0.79	B9V	R	83.78	0.644	83.23	0.703	0.47	1 / 1
2017.789	23189+0524	BU 80AB	8.18 / 9.39	1.21	K0	R	253.18	0.799	250.57	0.787	0.78	1 / 1
2017.789	23420+2018	STT 503AB	8.26 / 8.63	0.37	F8	R	134.03	1.051	134.34	1.047	0.26	1 / 1
2017.789	23455+2025	STT 505	6.75 / 9.61	2.86	G8III	R	59.72	2.386	60.11	2.394	2.38	1 / 1

Speckle Interferometry with the OCA Kuhn 22" Telescope - II

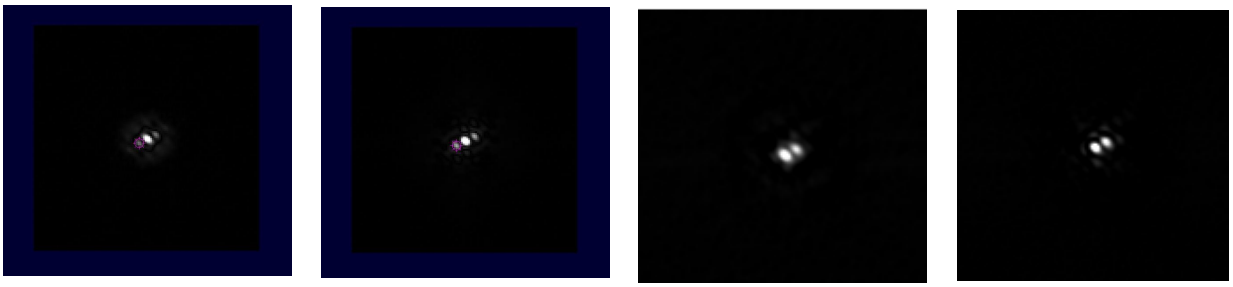

Figure 6. AC and BSA images of YR23, showing the smearing that arises from observation at too large a zenith angle. Left to right: AC in G filter, AC in R, BSA in G, BSA in R. Atmospheric dispersion appears to be greater in the G filter.

(Continued from page 278)

those from larger telescopes. It is likely that atmospheric dispersion also contributed to the scatter, because the star was observed at a zenith angle greater than 35 degrees. Both the AC and BSA measures, in both G and R filters, suffer from smearing by atmospheric dispersion, as seen in Figure 6.

The triple system **08044+1217 BU581ABC** is shown in Figure 7. In the autocorrelogram, the close AB components, which have nearly equal brightness, show multiple peaks when brightened enough to make the C component visible (~3 magnitudes fainter). In addition, the bright pair produces double peaks for C itself. The BSA image gives the proper view. The position angles of AB and AC happen to be nearly the same (Table 3). There are two entries in Table 3 for the same R filter, because this system was inadvertently observed twice in the same night. The WDS 45-year, grade 2 orbit for the AB pair has speckle observations covering nearly an entire orbit.

Figure 8 shows the binary star **09186+2049 HO43**, which has a recently-updated orbit solution (Tokovinin, 2016), with a period of 359 years. The new orbit relied heavily on recent accurate astrometry from Hipparcos, Tycho and speckle observations, which were rapidly departing from the previous (1989) orbit. The current points of Table 3 are in good agreement with the new orbit. Although Hipparcos data are generally considered more accurate than Tycho, in this case it may be that Tycho is favored because the components are slightly fainter than magnitude 9, the threshold for Hipparcos optimum accuracy.

The binary **10454+3831 HO532AC** is shown in Figure 9. It was observed in the IR742 filter because of the very red WDS spectral type (M2), and because of the large Δmagnitude (2.34). The red filter should reduce the magnitude difference if the secondary star is cooler (later type) than the primary, and indeed, the BSA Dmagnitude in Table 3 is 1.79. The WDS orbit plot is also shown in Figure 9, having a period of 161 years. However, based on inspection of historical data from the WDS Observation Catalog, together with the current observations, the orbit solution (Mante, 2000) is unlikely because some of the data points seem to be plotted in error. The WDS orbit ephemerides gives θ = 37 degrees (N-E quadrant) in 2017, but the bispectrum image shows that the secondary is currently in the opposite (S-W) quadrant, θ ~ 230 degrees (Table 3).

In Figure 9, the current AC and BSA points have

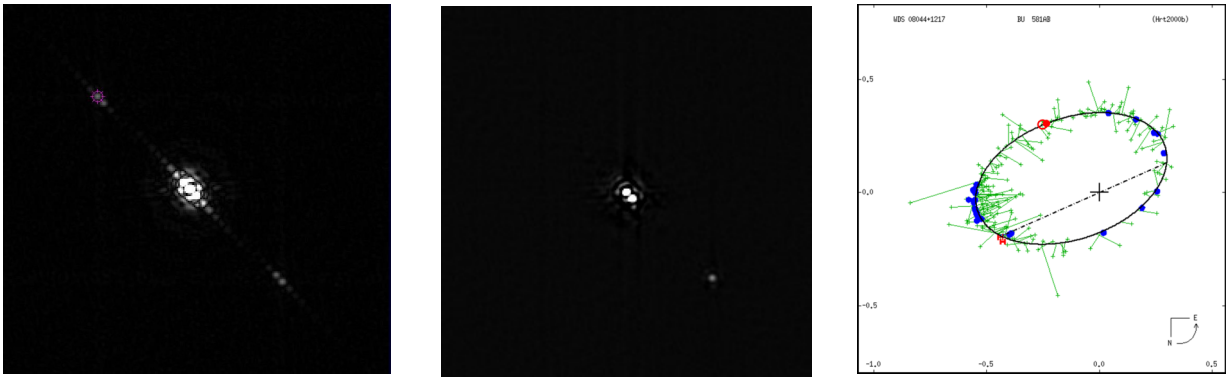

Figure 7. The triple system BU581ABC, observed in the R filter. Left and Middle: The autocorrelation and BSA reconstructed image, respectively. Right: The WDS orbit of the AB pair; Table 3 results are added as red circles - autocorrelation solid, and BSA open.

Speckle Interferometry with the OCA Kuhn 22" Telescope - II

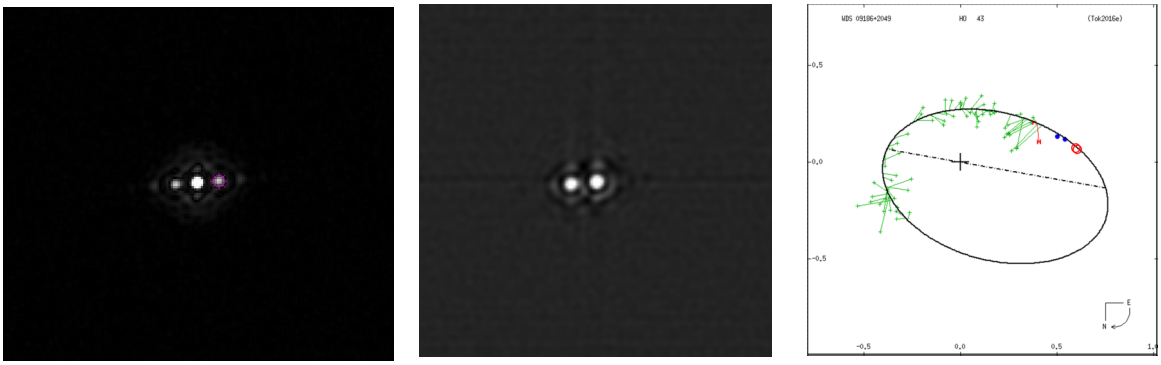

Figure 8. The binary HO43, observed in the R filter. Left: The autocorrelation. Middle: The BSA reconstructed image. Right: The WDS 2016 orbit, with Table 3 results added as red circles.

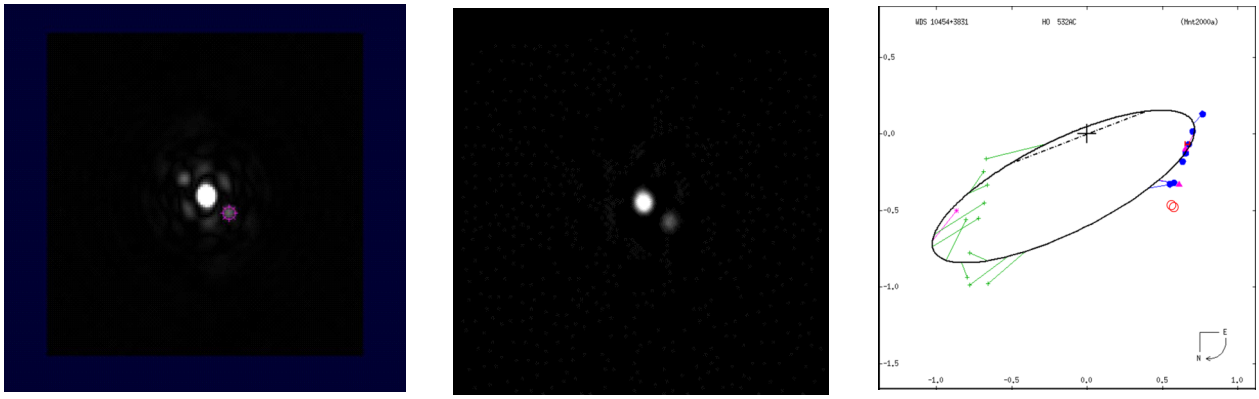

Figure 9. The HO532AC system. The AC and BSA image are at Left and Middle, respectively. Right: Orbit plot from the WDS 6th Orbit Catalog. The new AC and BSA points have been added as red circles. Note that these points (Table 3) were observed at θ ~ 230 deg, but that they are plotted in the opposite quadrant here (θ ~ 50 deg), to be consistent with the earlier plotted speckle points. The conclusion is that all the recent points in the orbit plot are in the wrong quadrant.

been added to the orbit plot, continuing the departure trend from the orbit solution; but note that they have been intentionally plotted in the opposite (N-E) quadrant (θ~50 deg), to appear consistent with the earlier plotted speckle points. The photographic, CCD and Hipparcos points, which don't show up well in the Figure because they happen to be nearly coincident with some speckle points, have also been plotted 180 degrees from their originally reported position angle; but these techniques have no θ ambiguity as AC does.

Figure 10 shows all data plotted with θ as *originally* reported in the WDS Observation Catalog, in a common North-up, East-left orientation. The visual micrometer data are all in the N-W quadrant, as in the orbit plot of Figure 9. However, the true locations of all recent data are 180 degrees from their Figure 9 locations – including the photographic and CCD points. The current AC and BSA points are plotted as given in Table 3, consistent with the bispectrum image.

In Figure 10 all the data fall together nicely, in both time sequence and position, forming a gently-curved

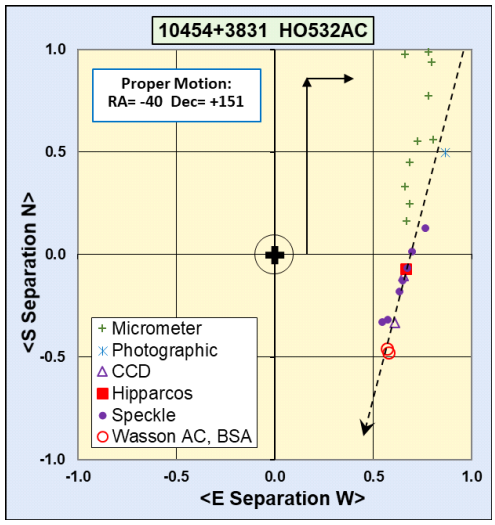

Figure 10. All observations of HO532AC from the WDS Observation Catalog. The solid arrows represent the WDS primary PM components in RA (-40) and Dec (+151), with an arbitrary scale. Their slope (dashed arrow) matches the astrometric points, however, the vectors would be much longer if scaled to the 121-year duration of the observations.

Speckle Interferometry with the OCA Kuhn 22" Telescope - II

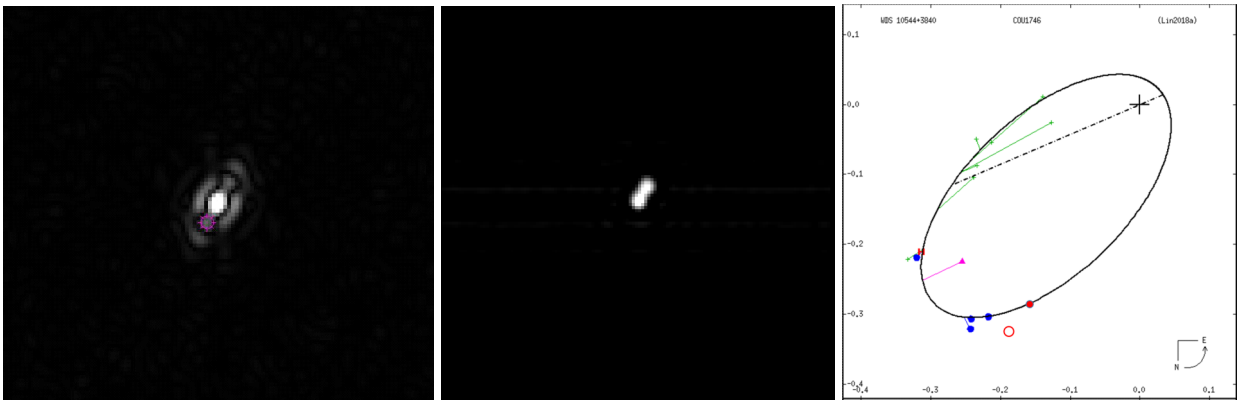

Figure 11. The COU1746 system observed with the IR742 filter. Left: AC. Middle: BSA reconstructed image. Right: WDS orbit plot, updated in 2018 based on three recent speckle points. The points from Table 3 are shown as red circles (AC open, BSA solid).

below the trend. The slope of the proper motion (PM) vectors, as shown in the Figure, happens to match the observations reasonably well. However, PM is given only for the primary star; if the faint star were far in the background, the primary PM would have carried the stars about 18" apart over the 121 years of observations, more than 10 times what has been observed. Therefore, the A and C components are probably traveling together, making HO532AC a true binary. It is recommended that a new orbit solution should be attempted, using the reported values of θ to correct the quadrant problem. However, a new orbit will evidently have a period much longer than 161 years.

10544+3840 COU1746, shown in Figure 11, was observed in the IR742 filter because it has late spectral type K0, is fairly faint, and the ephemerides from a previous orbit solution predicted ρ to be adequately wide (0.47"). However, consistent with the 2018 orbit update, it appears to be much closer (ρ < 0.4"), near or Rayleigh limit for the 844nm effective wavelength. Therefore, the AC has poor quality, and the BSA is not clearly resolved; for these reasons, the centroid peaks were uncertain, and both techniques were assessed as quality code 6 in Table 3. Even though the measurements are near the recently-updated orbit (Figure 11, right), they are not considered reliable.

The binary **11293+3025 L11** is seen in Figure 12. The IR742 IR-pass filter was used because of the large Δmagnitude of 3.13, together with adequately resolved separation. The primary spectral type is F6V (dwarf); therefore, the fainter secondary is probably a G or early K dwarf. As expected, the near IR-pass filter reduced the Dmagnitude somewhat, to 2.77. The Gaia satellite data release DR2 indicates this double is a close neighbor of the Sun, distance 67 parsecs, and the two components have similar PM.

The L11 orbit plot shows only one previous "speckle" data point, taken with the Palomar Observa-

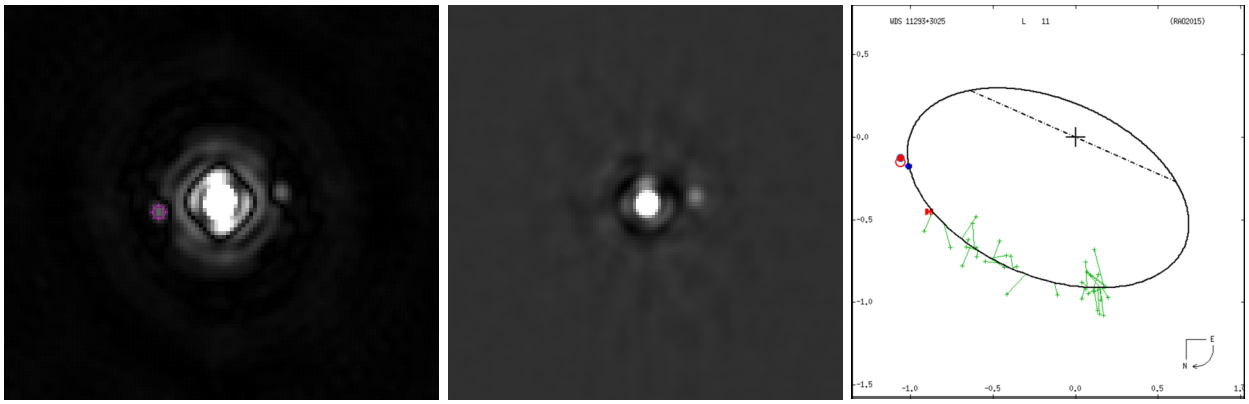

Figure 12. The binary 11293+3025 L11, observed with the IR742 filter. Left: AC, Middle: BSA reconstructed image. Right: WDS orbit plot, having only one previous speckle point. The data from Table 3 are red circles, AC open and BSA solid.

Speckle Interferometry with the OCA Kuhn 22" Telescope - II

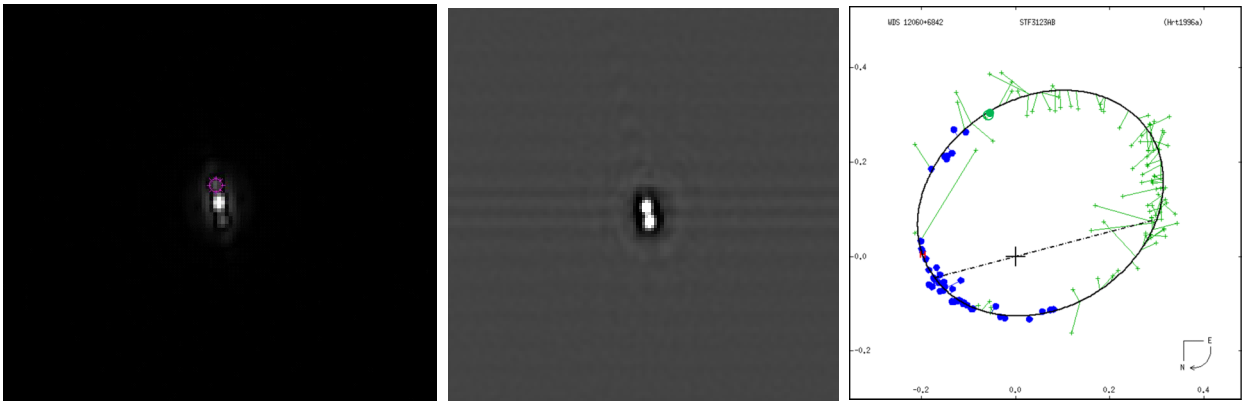

Figure 13. The binary 12060+6842 STF3123AB, observed with the G filter. Left: AC. Middle: BSA reconstructed image, highly stretched but not showing the C component. Right: WDS orbit plot for the AB pair, with data from Table 3 added as green circles, AC open and BSA solid.

tory 60-inch telescope, using the Robo-AO adaptive optics system (Riddle, et al, 2015). The new points from Table 3 are in reasonable agreement with it. This system is obviously in need of more speckle observations.

The **12060+6842 STF3123AB** binary is shown in Figure 13 in the G filter. Separation is close to the Rayleigh criterion (ρ ~ 0.24"), but the AB pair is reasonably well resolved. The BSA image (middle) is highly stretched, showing residual line pattern noise near the image floor, but still not revealing the C component. It is fortunate that the AB pair has had speckle observations throughout the periastron portion of its 122-year orbit.

The C component has only been observed six times before, beginning in 1885 with the Lick 36-inch refractor; the last observation, in 1924, used the 40-inch Yerkes refractor. In attempting to detect this star, which is extremely faint for speckle (WDS magnitude 15.7), the IR807 filter was used; it was assumed that if the C star is at the same distance as the AB pair, it could be a K or M dwarf. 4000 frames were taken with a long exposure (0.150 second), permitted because the seeing is much better at this long wavelength, but nearly saturating the AB stars.

The AC and BSA image results for the IR807 filter are seen in Figure 14. The AB pair is not fully resolved at the longer wavelength, and it is over-exposed when the images are highly stretched to reveal the faint C component. It is likely that C is much redder than the AB pair because it was detected in the near-IR but not in the visible (G) filter; in addition, the WDS Δ magnitude is 8.5 (probably V band), but it is reduced to about 5 in the IR807 filter. Although detection was successful, and it appears to be quite red, it is still not certain whether the C component is gravitationally bound to the AB binary. All observations of the C position are plotted in Figure 14, showing possible slow θ motion over more than 120 years.

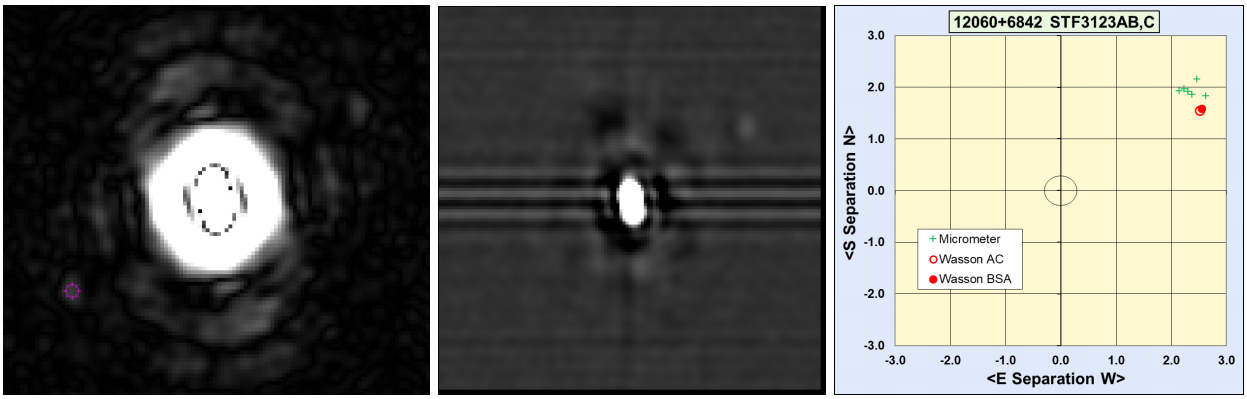

Figure 14. The binary 12060+6842 STF3123AB,C observed with the IR807 filter, and stretched to make the very faint C component visible. Left, AC. Middle: BSA reconstructed image. Right: All data plotted for the C component. The sx prior observations were made with micrometers on the world's two largest refractors.

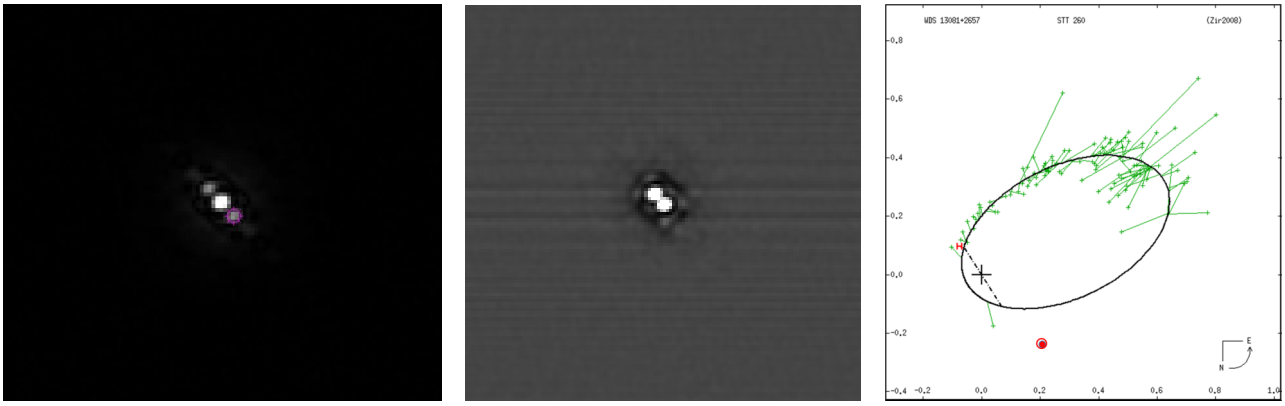

Figure 15. The binary 13081+2657 STT260 observed with the G filter. Left, AC. Middle, BSA reconstructed image. Right: WDS orbit plot with Table 3 speckle points added as red circles, AC (open) and BSA (solid).

The binary **13081+2657 STT260** was observed in the G filter, shown in Figure 15. It is unfortunate that there are no previous speckle observations, and that it was not observed with a large telescope during its recent periastron. The current AC and BSA observations are in good agreement, but they are far from the orbit ephemerides, possibly indicating a much longer period than the current 234-year orbit. Further observations are badly needed.

Acknowledgements

The author thanks Dave Rowe for his excellent Speckle Tool Box software, and particularly for the triple correlation bispectrum "tool," without which this work would not have been possible. In addition, he appreciates Rowe's WDS target-selection software, which simplifies and speeds target and reference star searches. He also thanks Russ Genet for his encouragement, correspondence, instruction and assistance along the speckle journey. The author is grateful to OCA President Barbara Toy for her dedication as custodian of the Kuhn 22-inch Telescope, and to the Orange County Astronomers for support and maintenance of the Anza site facilities. This research has made use of the Washington Double Star Catalog, the 6th Orbit Catalog, and the Observation Catalog, all maintained at the U.S. Naval Observatory, and the author particularly thanks Brian Mason for providing all previous observation data for the requested stars, and for his constructive comments.

This work has made use of data from the European Space Agency (ESA) mission Gaia (https://www.cosmos.esa.int/gaia), processed by the Gaia Data Processing and Analysis Consortium (DPAC, https://www.cosmos.esa.int/web/gaia/dpac/consortium). Funding for the DPAC has been provided by national institutions, in particular the institutions participating in the Gaia Multilateral Agreement.

References

Edelmann, Torsten, 2015. FireCapture2.4. http://firecapture.wonderplanets.de

Harshaw, Richard and Rowe, David and Genet, Russell, 2017. "The Speckle Toolbox: A Powerful Data Reduction Tool for CCD Astrometry." *Journal of Double Star Observations*, **13**, 52-67, January 1, 2017.

Horch, E., Ninkov, Z., van Altena, W. F., Meyer, R. D., Girard, T. M., and Timothy, J. G., 1999. *AJ*, **117**, 548.

Horch, E.P., Robinson, S.E., Ninkov, Z., van Altena, W.F., Meyer, R.D., Urban, S.E., Mason, B.D., 2002. *AJ,* **124**, 2245, 2002.

Losse, Florent, 2015. "REDUC 4.72." http://www.astrosurf.com/hfosaf.

Mante, R., 2000. *IAUDS Information Circulars*, **140**, 1, 2000.

Riddle et al, 2015. Riddle, R.L., Tokovinin, A., Mason, B.D., Hartkopf, W.I., Roberts, L.C., Jr., Baranec, C., Law, N.M., Bui, K., Burse, M.P., Das, H.K., Dekany, R.G., Kulkarni, S. Punnadi, S., Ramaprakash, A.N., & Tendulkar, S.P. *ApJ,* **799**, 4, 2015.

Rowe, David A. and Genet, Russell M., 2015. "User's Guide to PS3 Speckle Interferometry Reduction Program." *Journal of Double Star Observations*, **11**, 266-276.

Rowe, David A., 2016. Yahoo Group speckleinterferometry@yahoo.com.

Rowe, David A., 2017. Private communication.

Rowe, D., Genet, R., Wasson, R., 2019. In preparation for submittal to *JDSO*.

Serot, J., Wasson, R., Rowe, D., Genet, R., 2018. "Bispectrum-based Measurements of Close Large-Differential-Magnitude Visual Double Stars," *Journal of Double Star Observations*, **14-4**, 711-727, October 2018.

Sordiglioni, Gianluca, 2016. http://stelledoppie.goaction.it/index2.php?section=1.

Tokovinin, A., 2016. *ApJ,* **831**, 151, 2016.

Wasson, Rick, 2018. "Speckle Interferometry with the OCA Kuhn 22" Telescope," *Journal of Double Star Observations*, **14-2**, 223-241, April 2018.

Rick Wasson is a retired Aeronautical Engineer, who specialized in airplane aerodynamics throughout his career. He is a native of Southern California and has been an amateur astronomer since the age of 12 - about 6 decades. His astronomical interests include double stars, interferometry, photometry, asteroid occultations, and spectroscopy.